Anal. Chem. **1997,** *69,* 3708−3713

A Demonstration of Principal Component Analysis for EPR Spectroscopy: Identifying Pure Component Spectra from Complex Spectra

Oliver Steinbock,* Bettina Neumann,† Brant Cage, Jack Saltiel, Stefan C. Müller,† and Nar S. Dalal*

Department of Chemistry, Florida State University, Tallahassee, Florida 32306-3006

The application of principal component analysis (PCA) with self-modeling (SM) is extended to electron paramagnetic resonance (EPR) spectroscopy. Our approach develops a novel constraint in the SM procedure. This constraint relies on the mirror symmetry around the EPR peak position, a condition that is well satisfied by most paramagnetic compounds at the usual EPR measurement frequencies (9−10 GHz, the X-band). Examples considered are two- and three-component systems consisting of aqueous solutions of paramagnetic ions that exhibit distinct but overlapping spectra: Cu^{2+} (single peak), Mn^{2+} (sextet), and VO^{2+} (octet). The results show that the PCA technique is capable of reproducing the correct number of components and reconstructing spectra in good agreement with control measurements. Other spectroscopy areas to which the symmetric peak constraint should be applicable include NMR, NQR, and ICR.

A frequent problem in electron paramagnetic resonance (EPR) spectroscopy is the partial or complete overlap of signals from different paramagnetic species.[1] Consequently, the characterization, identification, and analysis of mixed EPR spectra is often difficult. Examples of this dilemma cover nearly the entire range of EPR applications, such as kinetic investigations of free radicals originating from chemical reactions[2] or radiolysis[3] and the analytical characterization[4] of the composition of paramagnetic inorganic, organic, and biological samples.[5] Related analyses[6] are sometimes even further complicated by the lack of information on the total number of paramagnetic species that result in a complex EPR signal and/or difficulties in obtaining the relevant pure substances that would allow the application of standard least-squares fitting procedures. One possible approach to help solve this problem is the use of higher frequencies and therefore higher magnetic fields.[7] High magnetic fields increase the separation of pure EPR signals, since the absorption maxima at H_0 shift according to the compound-specific *g*-values as expressed in

$$h\nu = g\beta H_0 \qquad (1)$$

where h is Planck's constant, ν denotes the microwave (or infrared) frequencies, and β is the Bohr magneton. Although high-field EPR spectrometers (ν > 100−400 GHz) are currently under development in some laboratories,[8] it is doubtful that these spectrometers will become standard analytical tools. We therefore see a need for improvements of analytical methodologies in the field of EPR spectroscopy.

Intriguing possibilities are opened by a technique known as principal component analysis (PCA),[9−11] which has found many applications in the field of optical spectroscopy. PCA has been used for the analysis of UV/visible and fluorescence data,[12,13] and its usefulness has also been demonstrated for liquid chromatography[14] and time-resolved infrared (FT-IR) spectroscopy.[15]

PCA has been applied to NMR spectroscopy.[16] In particular, Kvalheim[17] demonstrated that PCA is helpful in the assignment of the various peaks of a complex NMR spectrum, such as that from crude oil. PCA techniques were shown to be helpful in improving the quantitation of peak intensities in standard NMR as well as in NMR imaging.[18] To our knowledge, however, there has been no report of any application of PCA to EPR spectroscopy. In this context, we note that there are significant differences in the appearance and parameterization of NMR and EPR spectra. Whereas NMR spectra are recorded in the absorption mode, EPR peaks are measured in the derivative mode. Moreover, NMR spectra consist of many multiplets, each one representing a specific group of nuclei. In EPR, on the other hand, each peak arises from interaction of the unpaired electron with the whole paramagnetic entity. Thus the line shapes and routine analysis procedures differ for NMR and EPR spectroscopies. It follows

† Max-Planck-Institut für molekulare Physiologie, Rheinlanddamm 201, D-44147 Dortmund, Germany, and Otto-von-Guericke Universität, Institut für Experimentelle Physik, Universitätsplatz 2, D-39016 Magdeburg, Germany.

(1) (a) Barker, B. E.; Fox, M. E. *Chem. Soc. Rev.* **1980**, *9*, 143−84. (b) Ayscough, P. B. *Electron Spin Resonance in Chemistry*; Methuen: London, 1967.
(2) Neumann, B.; Steinbock, O.; Müller, S. C.; Dalal, N. S. *J. Phys. Chem.* **1996**, *100*, 12342−8.
(3) Box, H. C. *Radiation Effects: ESR and ENDOR Analysis*; Academic Press: New York, 1977.
(4) Dalal, N. S.; Suryan, M. M.; Seehra, M. S. *Anal. Chem.* **1981**, *53*, 938−40.
(5) Marsh, D. In *Biological Magnetic Resonance*; Berliner, L. J., Reuben, J., Eds.; Plenum Press: New York, 1989; Vol. 8, Chapter 5.
(6) Evans, J. C.; Morgan, P. H. *Anal. Chim. Acta* **1981**, *133*, 329−38.
(7) Brunel, L. C. *Appl. Magn. Reson.* **1992**, *3*, 83−97.
(8) Cage, B.; Hassan, A. K.; Pardi, L.; Krzystek, J.; Brunel, L. C.; Dalal, N. S. *J. Magn. Reson.* **1997**, *124*, 495−8.
(9) Beebe, K. R.; Kowalski, B. R. *Anal. Chem.* **1987**, *59*, 1007A−10A, 1012A, 1014A−7A.
(10) Sharaf, M. A.; Illman, D. L.; Kowalski, B. R. *Chemometrics*; Wiley: New York, 1986.
(11) Malinowski, E. R.; Howery, D. G. *Factor Analysis in Chemistry*; Wiley: New York, 1980.
(12) Sun, Y.-P.; Sears, D. F.; Saltiel, J. *Anal. Chem.* **1987**, *59*, 2515−9.
(13) Saltiel, J.; Sears, D. F.; Choi, Y.-O.; Sun Y.-P.; Eaker, D. W. *J. Phys. Chem.* **1994**, *98*, 35−46.
(14) Vandeginste, B.; Essers, R.; Bosman, T.; Reijnen, J.; Kateman, G. *Anal. Chem.* **1985**, *57*, 971−85.
(15) Hessling, B.; Souvignier, G.; Gerwert, K. *Colloq. INSERM* **1992**, *221*, 155−8. Hessling, B.; Souvignier, G.; Gerwert, K. *Biophys. J.* **1993**, *65*, 1929−41.
(16) Chemometrics Review, Fundamental Review Issue, *Anal. Chem.* **1996**, *68*, 21R−61R.
(17) Kvalheim, O. M.; Aksnes, D. W.; Brekke, T., Eide, M. O.; Sletten, E. *Anal. Chem.* **1985**, *57*, 2858−64.
(18) Stoyanova, R.; Kuesel, A. C.; Brown, T. R. *J. Magn. Reson., Ser. A* **1995**, *115*, 265−9.

S0003-2700(97)00308-9 CCC: $14.00

that the earlier demonstration of the utility of PCA to NMR[16,17] does not automatically imply its extension to EPR in a trivial way, and this conclusion provided the main motivation for undertaking the present investigation. The major goal was to demonstrate PCA for EPR spectroscopy and to evaluate its capabilities for solving related problems. For this purpose, a simple experimental model system was chosen, which consists of mixtures of two or three well-characterized,[19−22] noninteracting paramagnetic ions (Mn^{2+}, Cu^{2+}, VO^{2+}) in aqueous solution. EPR spectra of various mixtures were measured and analyzed by PCA using the standard self-modeling technique (originally suggested in ref 23) as well as a new approach which is based on the fact that EPR spectra have a mirror symmetry about the peak center. Specific goals of this study were to test the potential of these chemometric approaches to find the correct total number of paramagnetic species and to reconstruct the corresponding pure EPR spectra.

EXPERIMENTAL SECTION

All EPR measurements were made utilizing a Varian E-12 X-band (9.5 GHz) EPR spectrometer. The solutions were delivered by a gravity-driven flow system into a quartz flat cell (Wilmad) that was mounted in the EPR cavity and had an active volume of about 100 μL. All measurements were carried out at room temperature. Microwave power (20 mW) and magnetic field modulation amplitude (5.0 G) were adjusted for optimum intensity without line shape distortion. Spectra were measured over a range of 2000 G.

Sample and reference solutions of the following chemicals were prepared using doubly distilled water: $MnSO_4 \cdot H_2O$ (Fisher), $CuSO_4 \cdot 5H_2O$ (Fisher), and $VOSO_4 \cdot 3H_2O$ (Aldrich). Concentrations used for experiments on the two-component system were in the ranges of $[Mn^{2+}] = 0.5-2.5$ mM and $[Cu^{2+}] = 0.075-0.1$ M, and for the three-component system, $[Mn^{2+}] = 0.1-0.7$ mM, $[Cu^{2+}] = 1.0-8.0$ mM, and $[VO^{2+}] = 0.1-0.8$ mM. The spectra of the selected samples consisted of a simple peak (Cu^{2+}), a sextet (Mn^{2+}), and an octet (VO^{2+}).

EPR signal data were digitized on a Zenith Z-159 PC and transferred to a Pentium (90 MHz) PC for further processing. All analyses were performed using a newly developed software that utilizes optimized subroutines of the Windows-based MATLAB program (version 4.0). We tested our software by analyzing simulated, overlapping spectra of known types. The simulated spectra were in most cases generated as Gaussian functions. First-derivative EPR spectra were obtained by utilizing the difference method between successive points. We furthermore checked the robustness of our algorithms by repeating analyses after addition of random noise to the simulated spectra.

Mathematical Procedure. Principal component analysis is a powerful tool for the extraction of low-dimensional information from heavily overdetermined high-dimensional data.[12−14] A crucial requirement for its application is that the acquired experimental data are a linear combination of pure component signals. This requirement is obviously fulfilled for most EPR experiments. For an efficient use of the technique, it is also necessary that the ratios of all pure compounds vary between the acquisition of different spectra. In other words, a pair of compounds that appears with a constant ratio in all analyzed spectra, would be detected as one "pure" component. EPR spectroscopy, however, offers various possibilities to control signal ratios. Examples are the self-sustained and rate-dependent signal decay in kinetic EPR experiments (e.g., decay of radicals after irradiation) or naturally occurring concentration differences that are known to be present in most analytical problems (e.g., biological samples).

EPR spectra were measured over a 2000 G range. The corresponding signal intensities were digitized to 270 and 1080 equidistant points for the two- and three-component examples, respectively. In the following, this number will be denoted as n_0. Each spectrum can be considered as a n_0-dimensional vector containing the EPR signal in its usual first-derivative form. The first task is to integrate this intensity information along the field axis, since the present PCA application requires that the vectors consist of only non-negative values. In the case of EPR spectroscopy, one-time integration yields the microwave absorption spectrum of the detected paramagnetic species. A frequent complication in this procedure is that a nonzero baseline integrates (in the best case) to a linearly increasing offset. For aqueous solutions, such as those investigated here, nonzero baselines often result due to the high dielectric loss and to small leakage of the dispersion. To minimize this problem in a well-defined way, we calculated each spectrum's mean value and subtracted it from the original data. In addition, negative values in the integrated spectra (mainly caused by random noise during the measurement) were set to zero. After integration of the pretreated spectra, the corresponding absorbance vectors were normalized and piled up row by row to form a matrix $\mathbf{A} \in \mathbf{M}$ ($m_0 \times n_0$, R^+). The second moment matrix $\mathbf{M}$ of $\mathbf{A}$, also known as the covariance matrix, is then calculated by multiplication of the transpose of matrix $\mathbf{A}$ with $\mathbf{A}$ itself:

$$\mathbf{M} = \mathbf{A}^T\mathbf{A}, \quad \mathbf{M} \in \mathrm{M}\ (n_0 \times n_0, R^+) \tag{2}$$

Diagonalization of $\mathbf{M}$ yields eigenvalues and eigenvectors of the data. Provided that $n_0 \geq m_0$, n_0 eigenvalues λ_i are obtained. The eigenvalues are sorted in order of decreasing magnitude so that λ_α is the largest eigenvalue, λ_β is the second largest eigenvalue, and so forth. Two criteria are applied to judge the absolute number k ($k \leq m_0$) of pure components that contribute to the measured composite spectra: (a) the relative magnitude of the eigenvalues and (b) the fact that, in a k-component system, the $(k + 1)$th eigenvector is supposed to contain only random noise. This paper focuses on two- and three-component systems. A two-component system is identified when only the magnitudes of λ_α and λ_β are significant. When the magnitude of λ_γ (but not of λ_δ) is also significant, the spectral matrix $\mathbf{A}$ is a three-component system. The eigenvectors associated with λ_α, λ_β, and λ_γ are labeled as $\bar{\boldsymbol{V}}_\alpha$, $\bar{\boldsymbol{V}}_\beta$, and $\bar{\boldsymbol{V}}_\delta$, respectively and their contribution to the ith spectrum in $\mathbf{A}$, $\boldsymbol{S}_i$, is given by the combination coefficients α_i, β_i, and γ_i, respectively. $\bar{\boldsymbol{V}}_\delta$ contains essential information, $\gamma_i \neq 0$, for a three-component system, but contains only noise and does not contribute, $\gamma_i = 0$, for a two-component system. All the experimental spectra constituting a three-component matrix, and with the aid of self-modeling, the three pure component spectra are represented as points in the α, β, γ coordinate space.

For analytical purposes (i.e., compound identification), it would also be valuable to reconstruct EPR spectra of these k pure

(19) Bielski, B. H. J.; Gebicki, J. M. *Atlas of Electron Spin Resonance Spectra*; Academic Press: New York, London, 1967.
(20) Kumagai, H.; Ono, K.; Hayashi, H.; Abe, H.; Shimada, J; Shono, H.; Ibamoto, H. *Phys. Rev.* **1951**, *83*, 1077−7.
(21) Bugguley, D. M. S.; Bleaney, B.; Griffiths, J. H. E. *Proc. R. Soc. A* **1950**, *201*, 366−77.
(22) Hutchinson, C. A.; Singer, L. S. *Phys. Rev.* **1953**, *87*, 256−62.
(23) Lawton, W. H.; Sylvestre, E. A. *Technometrics* **1971**, *13*, 617−33.

compounds for further identification. Since it is usually reasonable to adapt the reconstruction process individually for the specific problem at hand, these details are given in the following two sections that present examples for two- and three component systems. Of general importance is the fact that, in a *k*-component system, projections of normalized spectra into the *k*-dimensional eigenvector space are confined within a $(k-1)$-dimensional linear subspace that is defined by the normalization constraint

$$\sum_{i=1}^{k} \mu_i \sum_{j=1}^{n_0} V_{ij} = 1 \qquad (3)$$

where μ_i denotes coordinates in the *k*-dimensional eigenvector space (e.g., $\mu_1 = \alpha$ and $\mu_2 = \beta$ for $k = 2$) and V_{ij} is the *j*th component of the *i*th eigenvector.

Two-Component System. For this study, we selected paramagnetic species with distinctly different spectra. These species were Cu^{2+} and Mn^{2+}. Cu^{2+} exhibits a singlet while Mn^{2+} yields a sextet due to hyperfine interaction ($I = {}^5/_2$). Aqueous solutions of various amounts of $MnSO_4$ and $CuSO_4$ were measured with the setup described in the Experimental Section. Three resulting examples of processed and integrated EPR spectra are shown in Figure 1a. Cu^{2+} is a spin $s = {}^1/_2$ and $I = {}^3/_2$ system yielding normally four absorption maxima that are, however, not resolvable in aqueous media. Mn^{2+}, on the other hand, shows a well-structured sextet and is, compared to Cu^{2+}, shifted to higher fields. The *g*-values of both ions are known to be g (Cu^{2+}) = 2.21 and g (Mn^{2+}) = 2.06.[17,18] Figure 1a shows three typical spectra from various Cu^{2+}/Mn^{2+} ratios. One can easily see that the major contribution arises from the Cu^{2+} ions, while Mn^{2+} only introduces four (and not six!) small peaks and a weak shoulder on the low-field side. The lowest field strength peak of Mn^{2+}, however, is completely hidden behind the relatively strong Cu^{2+} signal.

On the basis of these three composite spectra, the matrices **A** and **M** were generated and the corresponding eigenvalues and eigenvectors calculated. The inset of Figure 1b shows the two eigenvectors $\bar{\boldsymbol{V}}_\alpha$ and $\bar{\boldsymbol{V}}_\beta$ that correspond to the highest eigenvalues α and β, respectively. The main plot of Figure 1b depicts the two-dimensional eigenvector space in terms of its coordinates (α, β). The general idea of this representation is that each coordinate pair defines a spectrum $\bar{\boldsymbol{S}} = \alpha\bar{\boldsymbol{V}}_\alpha + \beta\bar{\boldsymbol{V}}_\beta$. Furthermore, since $\bar{\boldsymbol{V}}_\alpha$ and $\bar{\boldsymbol{V}}_\beta$ are orthonormal, each experimental spectrum $\boldsymbol{S}_i$ can be projected into the eigenvector space by calculation of its combination coefficients (α_i, β_i) from the following dot products:

$$\alpha_i = \boldsymbol{S}_i\bar{\boldsymbol{V}}_\alpha, \quad \beta_i = \boldsymbol{S}_i\bar{\boldsymbol{V}}_\beta \qquad (4)$$

Using this description, the analyzed mixture spectra are represented in Figure 1b by the closed circles. Two additional measurements with different concentration ratios (not used for analysis) are shown as open circles for further comparison. As is necessary for a real two-component system, all five experimental spectra correspond to points located on, or very close to, the normalization line defined by $\bar{\boldsymbol{V}}_\alpha$ and $\bar{\boldsymbol{V}}_\beta$ (eq 3, solid line in Figure 1b).

Two strategies were utilized for the determination of pure component spectra. The first one follows the self-modeling method originally suggested by Lawton and Sylvestre, which exploits the fact that absorption spectra consist of only non-negative values.[23,24] Since the pure compounds should furthermore be located on the normalization line, we can move along

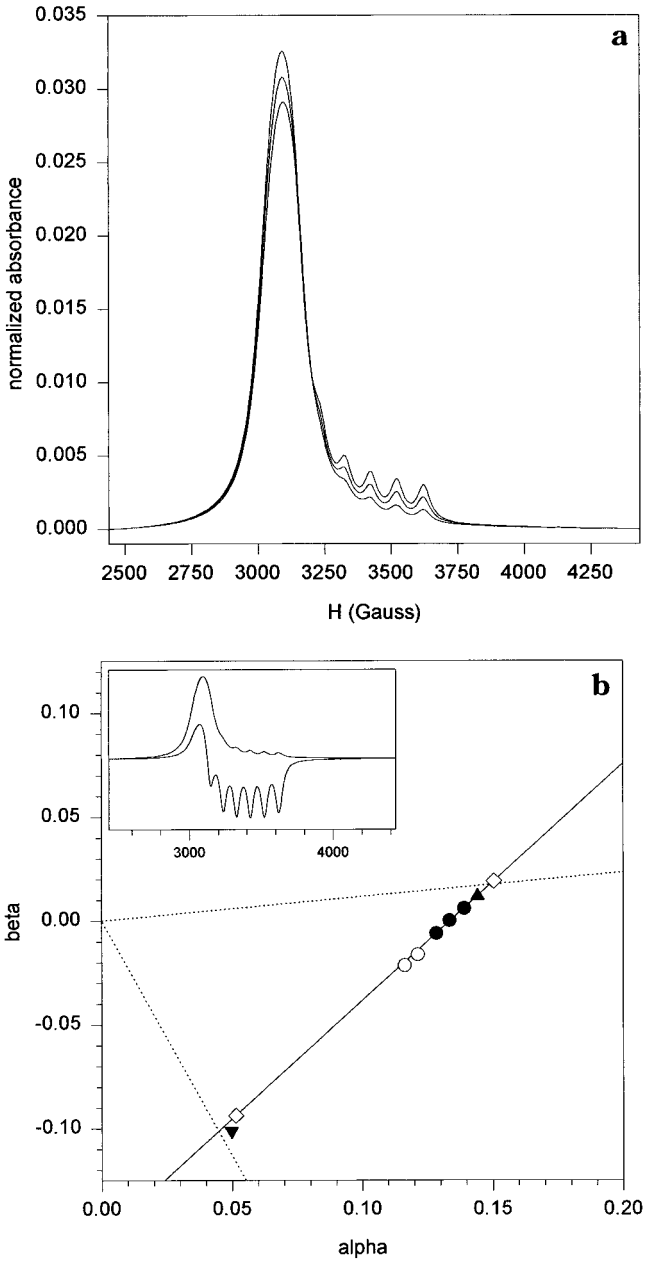

Figure 1. (a) Integrated and normalized EPR spectra of three aqueous solutions with the following concentration ratios of [$CuSO_4$] to [$MnSO_4$]: 190, 90, and 57. Note that two of the six manganese peaks are (partially) hidden under the higher Cu^{2+} absorbance. (b) Location of analyzed (●; compare spectra in (a)) and nonanalyzed mixed spectra (○) with respect to the coordinates (α, β) of the two-dimensional eigenvector space. All five points line up on the normalization line (solid line). The intersections of the dashed lines with the normalization line is at the Lawton−Sylvestre limits, while the two diamond symbols represent the position of pure spectra based on from the newly introduced EPR symmetry constraint (see text). For comparison, symbols ▲ and ▼ indicate the coordinates of pure Cu^{2+} and Mn^{2+}, respectively. The inset of (b) shows the eigenvectors $\bar{\boldsymbol{V}}_\alpha$ (upper curve) and $\bar{\boldsymbol{V}}_\beta$ (lower curve).

the line and determine the minimal absorption of each corresponding spectrum $\bar{\boldsymbol{S}}$. This self-modeling procedure is ideally applicable in cases such as ours, in which only one of the components contributes in certain spectral regions. In such cases, barring small uncertainties due to the experimental noise, the

(24) Sylvestre, E. A.; Lawton, W. H.; Maggio, M. S. *Technometrics* **1974**, *16*, 353−68.

outer limits of the Lawton and Sylvestre method yield exact pure component spectra.[12] However, as occasionally reported for other experimental applications, we experienced problems also in this EPR application. These problems arise from the unavoidable presence of noise and some systematic errors (e.g., concentration-dependent conductivity of ionic samples) in the experimental data which can shift the coordinates of the reconstructed pure spectra significantly. Problems of random noise are minimized by employing large experimental sets, a procedure purposely avoided in this work. To allow for random noise in the application of this self-modeling approach, it is therefore necessary to allow a certain margin for small negative values (here: absorbance minimum $> -5 \times 10^{-4}$ instead of >0).[12] The resulting Lawton and Sylvestre limits for the pure component spectra are shown in Figure 1b at the intersections of the dashed lines with the normalization line.

The second strategy helps obviate the above problem and utilizes the fact that EPR spectra of pure compounds exhibit, in contrast to most UV/visible spectra, mirror symmetry at a central field strength H_0^{sym}. This symmetry splits the signal into two parts, obeying the equation $A(H_0^{sym} + H) \approx A(H_0^{sym} - H)$. When a spectrum is in this sense reasonably symmetric, H_0^{sym} can be identified as

$$H_0^{sym} = \sum_{i=1}^{n_0} H_i A_i / \sum_{i=1}^{n_0} A_i \qquad (5)$$

where eq 5 gives the center of mass of the spectral peak. In our technique, we step along the normalization line, and for each step determine H_0^{sym} on the basis of eq 5, and then evaluate the symmetry of the corresponding spectrum by reflecting its low-field part onto its high-field part and calculating the root-mean-square (rms) deviation between the two parts. Figure 2a shows these rms values for spectra obtained along the normalization line of Figure 1b. The dotted curve in Figure 2a reveals two major minima at around $\alpha = 0.05$ and 0.15 and increasingly high values for $\alpha \rightarrow \pm\infty$. Since we expect mixed spectra to be of lower symmetry, the minima should identify good approximations of the combination coefficients of the pure spectra (Mn^{2+} and Cu^{2+}). The location of these recovered coordinates are shown as diamonds in Figure 1b. Notice also, the less significant local minima of the rms curve (Figure 2a) that most likely arise from the sextet structure of the Mn^{2+} spectrum. We emphasize that the new constraint relies on optimum symmetry in identifying pure component spectra, but it does not require that these spectra be perfectly symmetric.

Figure 2b shows the recovered spectra of the pure components (dashed and solid lines) and measured spectra of Mn^{2+} and Cu^{2+} (dotted lines), which are evidently in good agreement. They are also in good agreement with spectra reconstructed from the Lawton−Sylvestre limits (not shown). Additional analyses on the basis of four and five mixed spectra yielded for both techniques somewhat improved but nearly identical results to those shown in Figure 2b.

Three-Component System. To probe the analytical capabilities of PCA in EPR spectroscopy, we chose a three-component model system with the following paramagnetic ions: Mn^{2+}, Cu^{2+}, and VO^{2+}. The vanadyl ion VO^{2+} is an $s = {}^1/_2$, $I = {}^7/_2$ system, yielding an eight-line hyperfine spectrum in isotropic (liquid) media. The *g*-value of $VOSO_4$ in aqueous solution is known to be 1.96.

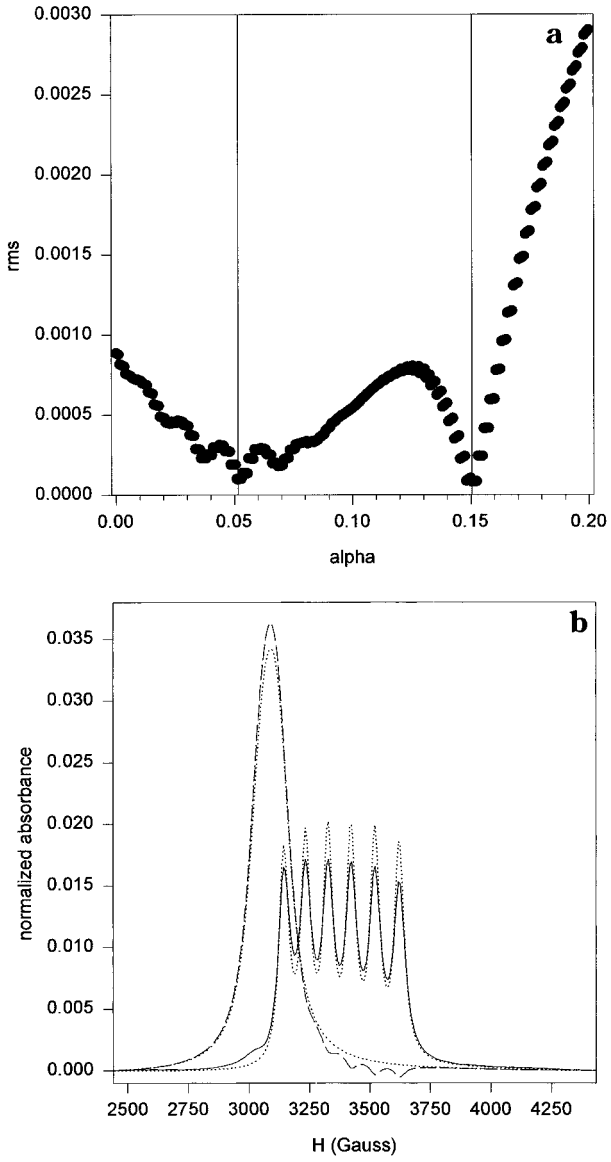

Figure 2. (a) Root-mean-square (rms) deviation between low- and high-field half of various theoretical spectra along the normalization line (see text). Points on the normalization line, $\alpha\Sigma\bar{\boldsymbol{V}}_{\alpha i} + \beta\Sigma\bar{\boldsymbol{V}}_{\beta i} = 1$, are represented by their α-value. The curve shows two major minima around $\alpha = 0.05$ and 0.15 (vertical solid lines), which correspond to the most mirror-symmetric solutions. (b) Comparison of integrated EPR signals of Mn^{2+} (solid line) and Cu^{2+} (dashed line) recovered on the basis of our symmetry considerations (cf. (a)) and experimentally measured pure spectra (dashed curves).

Figure 3a presents a typical EPR spectrum of an aqueous solution containing the three compounds. The spectrum is shown in the first-derivative and integrated forms. Analogous to the procedure used for the two-component system, an experimental matrix **A** of three normalized mixed spectra was generated and its second moment matrix diagonalized. In this case, we obtained three major eigenvalues with their three corresponding eigenvectors shown in the inset of Figure 3a. While in the case of a two-component system the normalization constraint (compare eq 3) defines a line, the three-component system is characterized by the arrangement of mixed-spectra coordinates on a plane. More precisely, all possible composite EPR signals should fall into a triangular, planar region after projection into their eigenvector space. Since the minimal requirement for the definition of a plane is the knowledge of three different points, it is obviously necessary

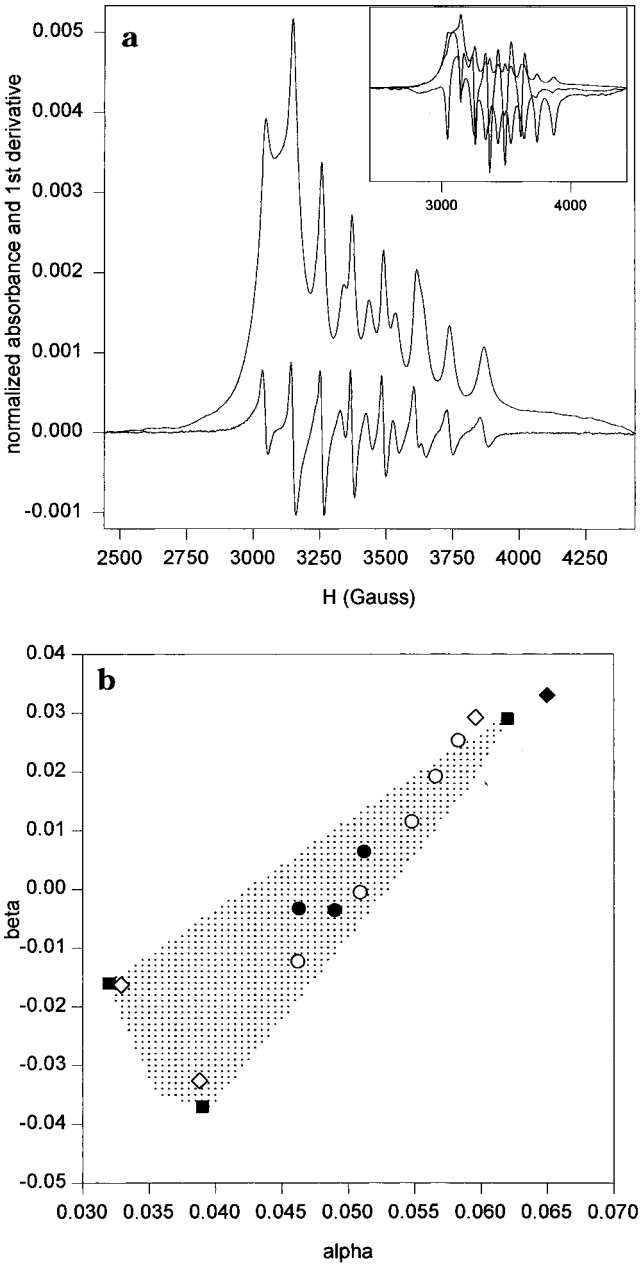

Figure 3. Measured EPR data and analysis results of a three-component aqueous system consisting of Mn^{2+}, Cu^{2+}, and VO^{2+} ions. (a) Typical example of a complex EPR spectrum (first derivative; lower curve) and its corresponding integration (absorbance; upper curve) was used in the PCA analysis. Concentrations: $[VOSO_4] = 0.8$ mM; $[MnSO_4] = 0.1$ mM; $[CuSO_4] = 1.0$ mM. The inset shows the three major eigenvectors obtained from the PCA of only three mixtures. (b) Projection of the corresponding three-dimensional eigenvector space in the (α, β)-plane. Symbols represent the coordinates of (●) analyzed EPR spectra, (○) additional EPR spectra of mixtures that were not used for the analysis shown here, (■) recovered spectra, (◆) most mirror-symmetric spectrum on the normalization plane and, for comparison, (◇) spectra of the three pure compounds, with Cu^{2+} in the upper left corner. The dotted triangular region covers coordinates that fulfill the Lawton−Sylvestre limit, which excludes reconstructed spectra with negative absorbance values (see text).

to analyze at least three different mixed spectra. When the matrix **A** is, however, limited to three experimental spectra for a three-component system, PCA is obviously pushed to its limits.

Figure 3b shows the projection of the three-dimensional eigenvector space into the (α, β)-plane. The coordinates of the three analyzed spectra are indicated by black dots. Five additional mixed spectra (not used for present analysis) are represented as open circles. It is noteworthy that the fact that the points are not located on a common line reemphasizes the presence of a third paramagnetic species in the mixture.

The combination of PCA with self-modeling, first developed by Lawton and Sylvestre for the resolution of two-component spectral mixtures, has been extended to three-component systems.[12,14,25−30] Borgen and Kowalski and Sun, Sears, and Saltiel have described extensions most directly related to the Lawton and Sylvestre approach. The relatively explicit latter extension[12] was employed in this work since it was developed and has been used in one of our laboratories for the resolution of unknown three-component spectral mixtures.[30] In contrast to two-component systems, three-component systems require a scan over a two-dimensional subspace (i.e., the normalization plane; compare eq 3). To simplify this analysis, it is useful to calculate the average coordinates of all analyzed projections and use these as a starting point for the scan. As in the case of the two-component system, we had to allow a small margin for negative values in order to apply the Lawton−Sylvestre non-negativity constraint. The coordinate region with (in the sense of Lawton−Sylvestre) proper absorbance $\bar{\boldsymbol{S}}_i = \alpha_i\bar{\boldsymbol{V}}_\alpha + \beta_i\bar{\boldsymbol{V}}_\beta + \gamma_i\bar{\boldsymbol{V}}_\gamma$ is indicated as the dotted triangle in Figure 3b. The coordinates of the three reconstructed spectra can then be located at the corner points of the triangle (solid squares in Figure 3b).

Application of the symmetry criterion, discussed above, reveals a complex two-dimensional function of rms values for the points on the normalization plane. The coordinate pair (α, β) of its global minimum is given as a solid diamond in Figure 3b. Its corresponding spectrum (not shown) is in good agreement with experimental data from pure Cu^{2+} solutions. The analysis of additional (local) minima is complicated in the present system, since the EPR signal of VO^{2+} in aqueous solution is rather asymmetric. Further analyses on the basis of symmetry considerations were therefore not performed.

Panels a−c of Figure 4 show the reconstructed EPR signals (solid lines) of the three pure components in their integrated form, with (a) VO^{2+}, (b) Cu^{2+}, and (c) Mn^{2+}. They can be seen to be in very good agreement with the additionally measured spectra of pure compound solutions (dashed lines). The signal-to-noise ratio of the integrated (absorbance) form of the reconstructed spectra is usually high enough to allow the calculation of low-noise derivative forms. As an example, Figure 4d shows the first derivatives of the Mn^{2+} spectra of Figure 4c. Sometimes, however, we encountered problems in obtaining satisfying derivative spectra, because small spikes in the absorption (reminiscent of very small contributions from other species; see also Figure 2b) are "magnified" by the calculation of derivatives. We found that this unexpected problem is caused most likely by small variations in the microwave resonance frequency of the EPR spectrometer. For most applications, however, this minor problem should be negligible or could be otherwise avoided by the use of appropriate standards.

(25) Ohta, N. *Anal. Chem.* **1973**, *45*, 553−7.
(26) Meister, A. *Anal. Chim. Acta* **1984**, *161*, 149−61.
(27) Sasaki, K.; Kawata, S.; Minami, S. *Appl. Opt.* **1984**, *23*, 1955−9.
(28) Delaney, M. F.; Mauro, D. M. *Anal. Chim. Acta* **1985**, *172*, 193−205.
(29) Vandeginste, B. G. M.; Leyten, F.; Gerritsen, M.; Noor, J. W.; Kateman, G.; Frank, J. *J. Chemom.* **1987**, *1*, 57−71.
(30) Borgen, O. S.; Kowalski, B. R. *Anal. Chem. Acta* **1985**, *174*, 1−26.
(31) Sun, Y.-P.; Sears, D. F., Jr.; Saltiel, J.; Mallory, F. B.; Mallory, C. W.; Buser, C. A. *J. Am. Chem. Soc.* **1988**, *110*, 6974−84.

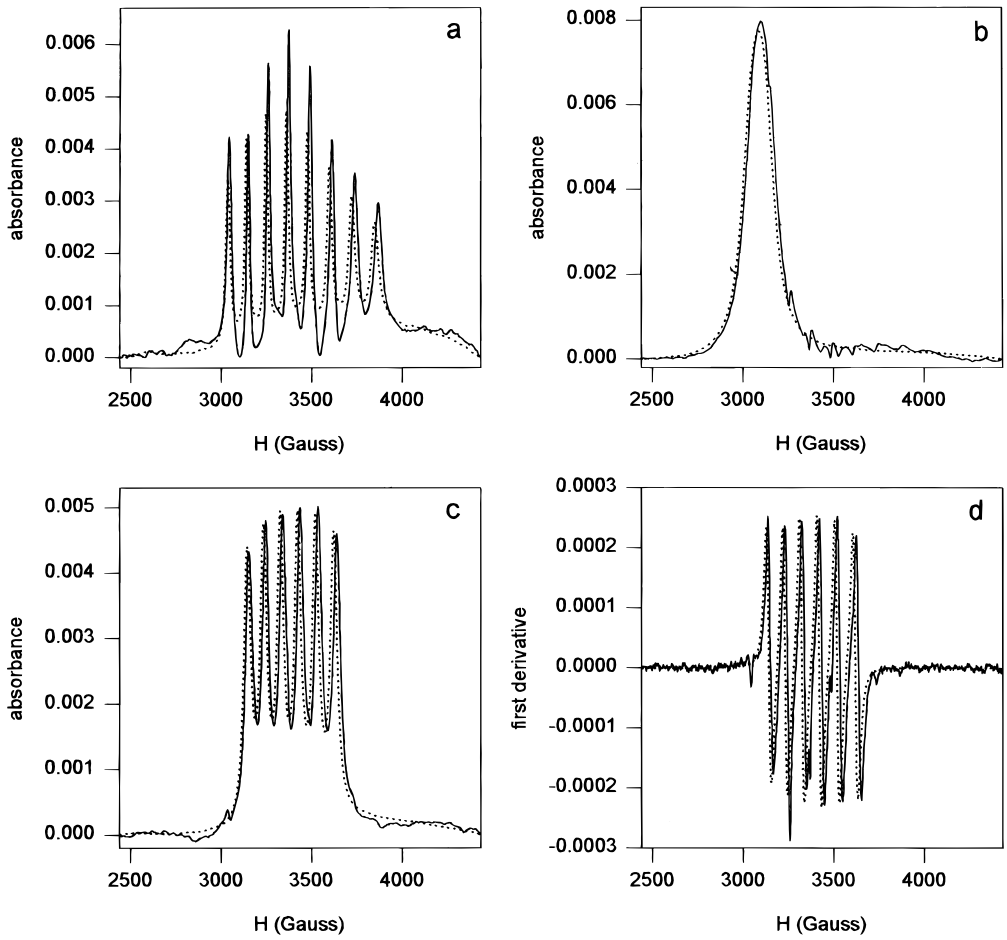

Figure 4. Recovered spectra (solid lines) of VO^{2+} (a), Cu^{2+} (b), and Mn^{2+} (c), and additionally measured pure spectra (dotted lines) in the integrated (absorbance) form. The first derivative form of the recovered and directly measured Mn^{2+} spectrum (dotted and solid lines, respectively) are shown in (d).

DISCUSSION

On the basis of the good agreement between the experimentally observed and theoretically reconstructed spectra, we conclude that the PCA technique can be adapted easily to analysis of multicomponent EPR spectra. A new self-modeling constraint introduced here, which is specific to magnetic resonance spectra, is the inclusion of line shape symmetry in the search for pure components. This additional constraint has indeed been found to be helpful in reaching a more stringent convergence to the resolution of the superposed spectra into their constituent components. It can be noted that this constraint is quite generally valid because under normal conditions magnetic resonance signals exhibit either a Gaussian or Lorentzian shape and are therefore symmetric about their mean positions. It is expected that this newly added feature will prove to be a valuable part of the PCA technique as applied to cases where strongly overlapping spectra are inherently symmetric, as they are in magnetic resonance.

The present study was an attempt to explore the analytical potential of the PCA procedure in EPR spectroscopy, wherein complex spectra due to superposition of multiple components is not uncommon. In our own studies in chemical kinetics, we have experienced difficulties in distinguishing between the assignments of complex EPR signals to hyperfine multiplets versus a superposition of signals from two or more free radicals.[2] Similarly, our earlier studies on the identification of γ-ray-induced free radical formation in hydrogen-bonded ferroelectrics have been hampered by our inability to analyze the observed multitude of the peaks in the EPR spectra especially in the $g = 2.00$ region.[32] The EPR spectra of fossil fuels are also complex and their definitive assignment still remains unsolved, although very high frequency measurements have been helpful.[33] It is felt that in all such cases the availability of a technique such as described here could constitute an important aid in the spectral assignment. Other intriguing possibilities are opened by the parallel use of optical and EPR spectroscopy in combination with principal component analysis: By using spectral matrices whose rows are composed of both EPR and UV/visible absorption spectra, the ability to resolve the composite EPR spectra can be exploited in resolving strongly overlapping optical spectra.

ACKNOWLEDGMENT

This work was supported by the U.S. Bureau of Mines, the Florida State University, and the Deutsche Forschungsgemeinschaft. J.S. thanks the National Science Foundation for a grant. Fruitful discussions with Donald Sears are gratefully acknowledged. O.S. thanks the Fonds der Chemischen Industrie for a Liebig Fellowship.

Received for review March 19, 1997. Accepted July 5, 1997.[⊗]
AC970308H

(32) Dalal, N. S. *Adv. Magn. Reson.* **1982**, *11*, 119−215.
(33) Dalal, N. S.; Smirnov, A.; Belford, L. *Appl. Spectrosc.*, in press.

[⊗] Abstract published in *Advance ACS Abstracts,* August 15, 1997.